

Energies of I⁸⁺ through I¹²⁺ low-lying levels

Karol Kozioł*, Jacek Rzadkiewicz

Narodowe Centrum Badań Jądrowych (NCBJ), Andrzeja Sołtana 7, 05-400 Otwock-Świerk, Poland

Abstract

High-accuracy Multi-Configuration Dirac–Hartree–Fock with Configuration Interaction calculations of level energies and transition rates have been carried out for iodine I⁸⁺ through I¹²⁺ ions related to the [Kr]4d^{*n*} (*n* = 5–9) configurations. For I¹⁰⁺ through I¹²⁺ ions the present data fill up the lack of such data in the literature.

*Corresponding author.

Email address: E-mail: karol.koziol@ncbj.gov.pl (Karol Kozioł)

Contents

1. Introduction	2
2. Theoretical background	3
3. Results	4
3.1. Probing the convergence of MCDHF-CI calculations	4
3.2. Estimating theoretical uncertainties	4
3.3. Comparing to experiments	6
References	7
Explanation of Tables	9
Tables	
1. I ⁸⁺ levels, 4d ⁹ valence electronic configuration (Rh-like ion)	10
2. I ⁹⁺ levels, 4d ⁸ valence electronic configuration (Ru-like ion)	11
3. I ¹⁰⁺ levels, 4d ⁷ valence electronic configuration (Tc-like ion)	12
4. I ¹¹⁺ levels, 4d ⁶ valence electronic configuration (Mo-like ion)	13
5. I ¹²⁺ levels, 4d ⁵ valence electronic configuration (Nb-like ion)	15
6. M1 transition for I ⁸⁺ ion	18
7. Selected M1 transitions for I ⁹⁺ ion	19
8. Selected M1 transitions for I ¹⁰⁺ ion	20
9. Selected M1 transitions for I ¹¹⁺ ion	22
10. Selected M1 transitions for I ¹²⁺ ion	26

1. Introduction

The spectroscopic properties of high-charged ions (HCIs) with the open d shell are widely utilized in fields such as astronomy and plasma physics. The presence of open d shells leads to the existence of numerous atomic levels and radiative transitions. Recent study suggested that HCIs with $d^{(4-6)}$ configurations might host suitable forbidden transitions for optical-clock frequency measurements [1]. The low-lying states related to the $(n = 4 - 5)d^6$ and $(n = 4 - 5)d^8$ configurations has been analyzed by Yu and Sahoo [2] for a series of ions across Mo-like, W-like, Ru-like, and Os-like isoelectronic sequences in order to identify transitions that can be suitable for making single-ion-based optical clocks, however iodine ions have been not considered in that study. Indeed there is a lack of data for energy levels of iodine ions with intermediate charge in the National Institute of Standards and Technology Atomic Spectra Database (NIST ASD) [3]. The spectrum of I IX has been analyzed by Joshi et al. [4] and then by Churilov et al. [5]. The spectrum of I X has been analyzed by Gayasov et al. [6] and then also by Churilov et al. [5]. Ivanova [7] provided calculations for the fine structure energy splitting $[\text{Kr}]4d^9\ ^2D_{5/2} - ^2D_{3/2}$ for Rh-like ions with $52 \leq Z \leq 86$, including iodine ion. Unfortunately there is no detailed analysis of the I XI, I XII, and I XIII spectra in the literature. Here we present the high-accuracy calculations of, employing the Multi-Configuration Dirac–Hartree–Fock (MCDHF) method with Configuration Interaction (CI), of energy levels and transition rates between them for $[\text{Kr}]4d^n$ ($n = 5 - 9$) configurations for I⁸⁺ through I¹²⁺ ions.

2. Theoretical background

The calculations of the radiative transition energies and rates have been carried out by means of the GRASP2018 [8] code. The GRASP2018 code is based on the MCDHF method. The methodology of MCDHF calculations performed in the present study is similar to that published earlier in many papers (see, e.g., [9, 10]). The effective Hamiltonian for an N -electron system is expressed by

$$H = \sum_{i=1}^N h_D(i) + \sum_{j>i=1}^N C_{ij}, \quad (1)$$

where $h_D(i)$ is the Dirac operator for the i th electron and the terms C_{ij} account for the electron–electron interactions. In general, the latter is a sum of the Coulomb interaction operator and the transverse Breit operator. An atomic state function (ASF) with total angular momentum J and parity p is assumed in the form

$$\Psi_s(J^p) = \sum_m c_m(s) \Phi(\gamma_m J^p), \quad (2)$$

where $\Phi(\gamma_m J^p)$ are the configuration state functions (CSFs), $c_m(s)$ are the configuration mixing coefficients for state s , and γ_m represents all information required to define a certain CSF uniquely. The CSFs are linear combinations of N -electron Slater determinants which are antisymmetrized products of 4-component Dirac orbital spinors. In the GRASP2018 code, the Breit interaction contribution to the energy (calculated in low-frequency limit) is added perturbatively, after the radial part of wavefunction has been optimized. Also two types of quantum electrodynamics (QED) corrections: the self-energy (as the screened hydrogenic approximation [11] of the data of Mohr and co-workers [12]) and the vacuum polarization (as the potential of Fullerton and Rinker [13]) have been included. The accuracy of the wavefunction depends on the CSFs included in its expansion [14, 15]. The accuracy can be improved by extending the CSF set by including the CSFs originating from excitations from orbitals occupied in the reference CSFs to unfilled orbitals of the active orbital set (i.e., CSFs for virtual excited states). This approach is called Configuration Interaction (CI). The CI method makes it possible to include the major part of the electron correlation contribution to the energy of the atomic levels. In the CI approach, it is very important to choose an appropriate basis of CSFs for the virtual excited states. It can be done by systematically building CSF sequences by extending the Active Space (AS) of orbitals and concurrently monitoring the convergence of the self-consistent calculations.

Table A

Active spaces of CSFs used in calculations.

Active space	Virtual orbitals	Number of CSFs				
		I ⁸⁺	I ⁹⁺	I ¹⁰⁺	I ¹¹⁺	I ¹²⁺
AS0		2	9	19	34	37
AS1	4f + $n = 5$, $l = 0-5$	13329	80991	199886	302780	316733
AS2	4f + $n = 5-6$, $l = 0-5$	42778	258780	636743	958366	993778
AS3	4f + $n = 5-7$, $l = 0-5$	88907	536698	1318954	1980512	2047144

The active spaces used in calculations for particular iodine ions are presented in Table A. The AS0 is a multi-reference (MR) CSFs set. The MR configurations are [Kr]4d n where $n = 9, 8, 7, 6, 5$ for I⁸⁺, I⁹⁺, I¹⁰⁺, I¹¹⁺, I¹²⁺ ions respectively. We have

considered all possible single (S) and double (D) substitutions from the 4s, 4p, 4d occupied subshells to the active space of virtual orbitals. In this case, the inactive core contains $n = 1, 2, 3$ shells. In our calculations we used the active spaces of virtual orbitals with n up to $n = 7$ and l up to $l = 5$. From Table A one can conclude that: (i) the number of CSFs increases rapidly when active space grows, reaching $\sim 2 \times 10^6$ CSFs for AS3 for I^{11+} ($4d^6$) and I^{12+} ($4d^5$) ions, and (ii) the size of the expansions increases with the size of the reference set.

3. Results

3.1. Probing the convergence of MCDHF-CI calculations

Figures 1 and 2 present the convergence in MCDHF-CI calculations for levels of I^{8+} and I^{9+} ions. The energy values presented therein are the level energies relative to the absolute energy of the ground state calculated at the MR stage, i.e. $\tilde{E}(\text{state}\#x, \text{ASy}) = E(\text{state}\#x, \text{ASy}) - E(\text{state}\#1, \text{MR})$. Looking at Figures 1 and 2 one can claim that the AS3 stage is adequate to achieve level energy convergence. The convergence of MCDHF-CI calculations near to the AS3 stage is clearer visible when considering energies relative to the groundstate, i.e. $\bar{E}(\text{state}\#x, \text{ASy}) = E(\text{state}\#x, \text{ASy}) - E(\text{state}\#1, \text{ASy})$ – see Figures 3, 4, and 5 for the cases of selected states of I^{8+} and I^{9+} ions.

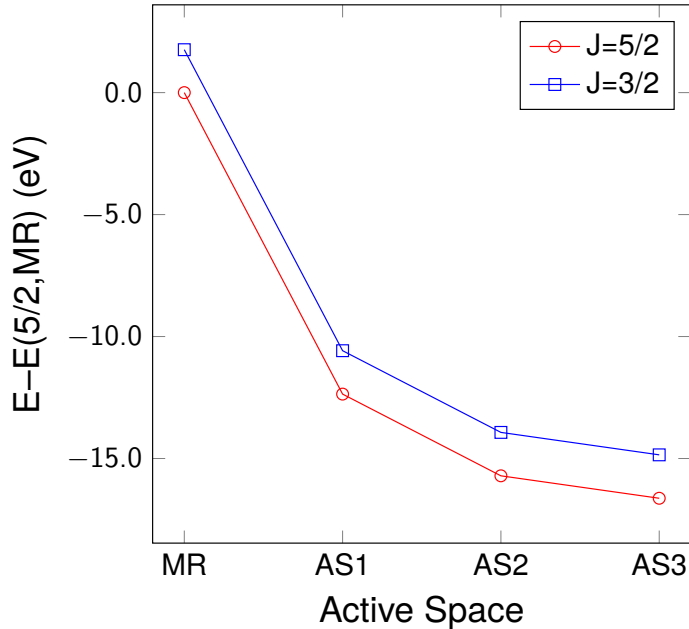


Fig. 1: Level energy convergence in CI calculation for I^{8+} – shifted absolute energies.

3.2. Estimating theoretical uncertainties

The theoretical uncertainties of level energies are related to convergence with the size of a basis set and estimated as absolute value of difference between energies calculated within AS2 and AS3, i.e. $\delta E = |E^{\text{AS3}} - E^{\text{AS2}}|$. Such an estimation gives 0.8 cm^{-1} (0.005%) uncertainty for the energy of ${}^2\text{D}_{5/2} - {}^2\text{D}_{3/2}$ splitting in I^{8+} , up to 0.3% uncertainty for theoretical level energies of I^{9+} and I^{10+} ions, and up to 0.5% uncertainty for theoretical level energies of I^{11+} and I^{12+} ions. The theoretical uncertainties of transition rates were estimated according to the procedure described by Kramida [16]. Among all M1 transitions for given ion, the subset of

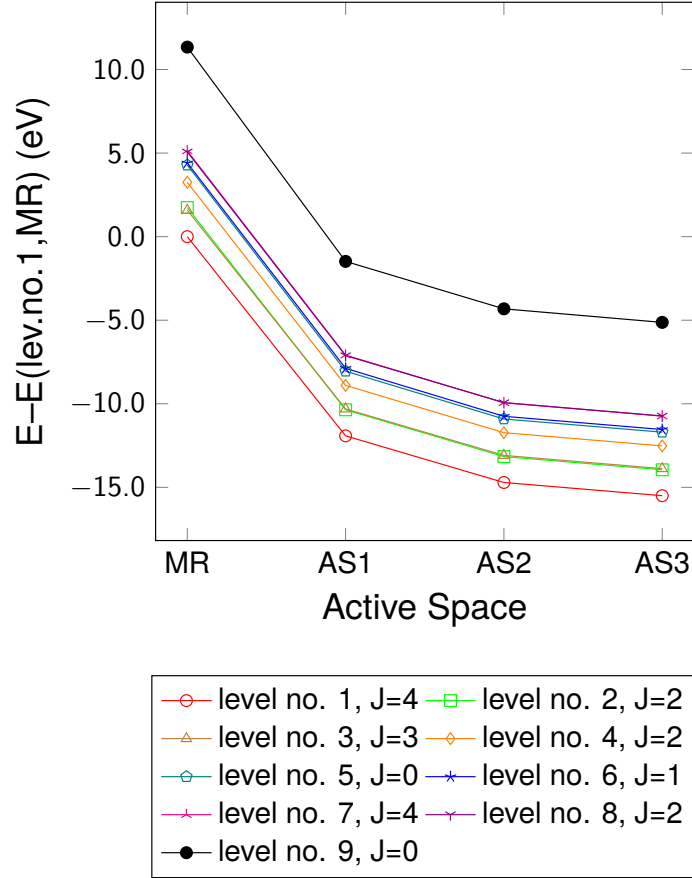


Fig. 2: Level energy convergence in CI calculation for I^{9+} – shifted absolute energies.

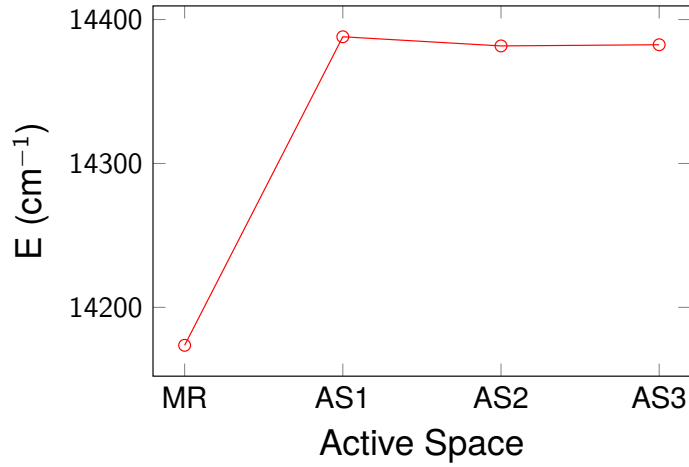


Fig. 3: Level energy convergence in CI calculation for $J = 3/2$ level of I^{8+} – relative energy.

high-intensity transitions (with the intensities higher than 10% of the strongest transition intensity) has been selected for estimating transition rate uncertainty, i.e. $\delta A = |A^{AS3} - A^{AS2}|$. The obtained value of uncertainty has been extended to all studied transitions. Such an estimation gives $\approx 0.02\%$ uncertainty for transition rate of $^2D_{5/2} - ^2D_{3/2}$ transition in I^{8+} and $\approx 0.3\%$ uncertainty for all transition rates of I^{9+} , I^{10+} , I^{11+} , I^{12+} ions.

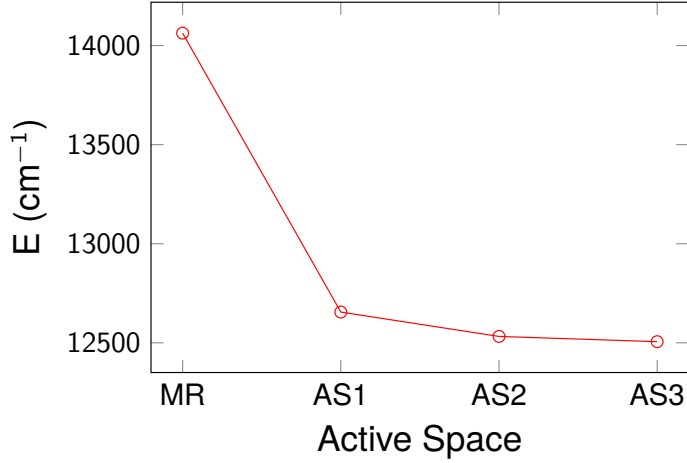


Fig. 4: Level energy convergence in CI calculation for the level no. 2 of I^{9+} – relative energy.

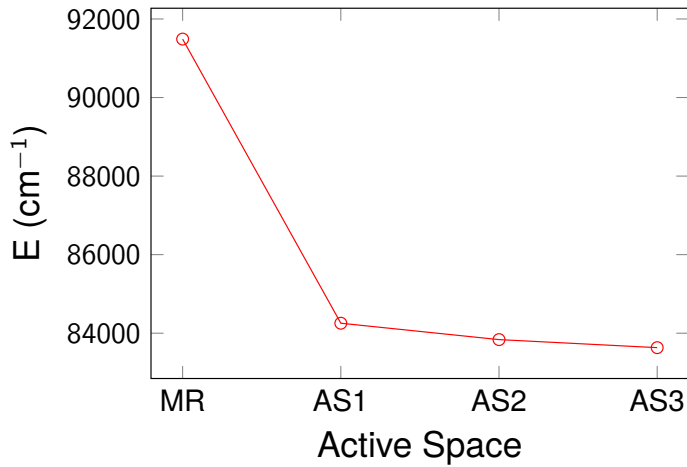


Fig. 5: Level energy convergence in CI calculation for the level no. 9 of I^{9+} – relative energy.

Where there are no reference values to which the calculated numbers can be compared to, the comparison between numbers calculated by two different methodologies can be used to estimate the theoretical differences for the transition rates. Table B presents the values for three strongest M1 transition rates for each I ion (except for I^{8+} , for which only one transition is analyzed), calculated by means of the GRASP2018, based on the MCDHF method, and by means of the FAC code [17], based on the multiconfigurational Dirac–Hartree–Fock–Slater (MCDHFS) method. The factor $|\Delta| = |(A^{\text{GRASP}} - A^{\text{FAC}})/A^{\text{GRASP}}|$ evaluates the difference between GRASP2018 and FAC results. One can see from Table B that the transition rates for I^{8+} , I^{9+} , and I^{10+} ions have B accuracy class (uncertainties $\leq 10\%$), according to accuracy categorization introduced in the NIST ASD, while the transition rates for I^{11+} and I^{12+} ions have C+ accuracy class (uncertainties $\leq 18\%$).

3.3. Comparing to experiments

Present MCDHF-CI calculated energy levels for $4d^9$ valence electronic configuration of I^{8+} ion and $4d^8$ valence electronic configuration of I^{9+} ion compared to the ones deduced from experimental spectra are presented in Tables C and D. As one can see the theory-experiment difference does not exceed 2.6%. Basing on this finding and on theoretical uncertainties presented in

Table B

High-intensity M1 transitions selected for estimating transition rate uncertainty, by comparing the GRASP2018 and the FAC calculated numbers.

Ion	Transition	Transition rate (s^{-1})		$ \Delta $ (%)
		GRASP	FAC	
I ⁸⁺	$^2\text{D}_{5/2} - ^2\text{D}_{3/2}$	48.09	45.29	5.8
I ⁹⁺	$^1\text{S}_0 - ^3\text{P}_1$	637.21	655.31	2.8
I ⁹⁺	$^1\text{D}_2 - ^3\text{F}_3$	105.33	98.76	6.2
I ⁹⁺	$^3\text{F}_3 - ^3\text{F}_4$	56.32	51.46	8.6
I ¹⁰⁺	$^2\text{D}_{5/2} - ^4\text{F}_{7/2}$	222.86	223.77	0.4
I ¹⁰⁺	$^2\text{D}_{3/2} - ^2\text{D}_{5/2}$	177.43	162.52	8.4
I ¹⁰⁺	$^2\text{D}_{5/2} - ^4\text{P}_{5/2}$	162.10	164.99	1.8
I ¹¹⁺	$^1\text{S}_0 - ^3\text{P}_1$	765.77	764.77	0.1
I ¹¹⁺	$^3\text{P}_0 - ^3\text{D}_1$	313.55	306.29	2.3
I ¹¹⁺	$^3\text{P}_0 - ^3\text{D}_1$	299.43	250.88	16.2
I ¹²⁺	$^4\text{F}_{5/2} - ^4\text{G}_{5/2}$	258.74	295.83	14.3
I ¹²⁺	$^2\text{P}_{1/2} - ^2\text{S}_{1/2}$	212.57	226.43	6.5
I ¹²⁺	$^2\text{F}_{5/2} - ^4\text{F}_{5/2}$	177.18	198.28	11.9

Table C

Comparison of present MCDHF-CI calculation results for [Kr]4d⁹ $^2\text{D}_{5/2} - ^2\text{D}_{3/2}$ energy splitting in I⁸⁺ ion to the experimental data found in the literature. Relative difference between theoretical and experimental data, given as $\Delta = (\text{Theo.} - \text{Exp.})/\text{Exp.}$ is also reported.

Theoretical (cm^{-1})	Experimental (cm^{-1})	Ref.	Δ (%)
14382.51	14362	[4]	0.1
	14392.77	[18]	-0.1

Section 3.2 we roughly estimate the uncertainties for energy levels for I⁹⁺ through I¹²⁺ to be 3% (A accuracy class).

References

- [1] C. Lyu, C. H. Keitel, and Z. Harman, (2023), arXiv:2305.09603 .
- [2] Y.-M. Yu and B. K. Sahoo, *Physical Review A* **109**, 023106 (2024).
- [3] A. E. Kramida, Y. Ralchenko, J. Reader, and N. A. Team, *NIST Atomic Spectra Database*, (version 5.12), [Online]. Available: <https://physics.nist.gov/asd> [Thu Dec 05 2024]. National Institute of Standards and Technology, Gaithersburg, MD (2024).
- [4] Y. N. Joshi and T. A. M. van Kleef, *Journal of the Optical Society of America* **70**, 1344 (1980).

Table D

Present MCDHF-CI calculated energy levels for 4d⁸ valence electronic configuration of I⁹⁺ ion compared to the ones deduced in Ref. [5] from experimental spectra. Relative difference between theoretical and experimental data, given as $\Delta = (\text{Theo.} - \text{Exp.})/\text{Exp.}$ is also reported.

<i>J</i>	Theoretical (cm ⁻¹)	Experimental (cm ⁻¹), Ref. [5]	Δ (%)
4	0.0	0	–
2	12505.90	12230	2.3
3	13051.94	13043	0.1
2	24030.07	23854	0.7
0	30638.93	29860	2.6
1	31967.99	31440	1.7
4	38430.16	37503	2.5
2	38488.11	38198	0.8
0	83632.17	81670	2.4

- [5] S. S. Churilov, Y. N. Joshi, and R. R. Gayazov, *Journal of the Optical Society of America B* **15**, 1923 (1998).
- [6] R. R. Gayasov, S. S. Churilov, Y. N. Joshi, A. N. Ryabtsev, and V. I. Azarov, *Journal of the Optical Society of America B* **14**, 1013 (1997).
- [7] E. P. Ivanova, *Atomic Data and Nuclear Data Tables* **95**, 786 (2009).
- [8] C. Froese Fischer, G. Gaigalas, P. Jönsson, and J. Bieroń, *Computer Physics Communications* **237**, 184 (2019).
- [9] K. G. Dyall, I. P. Grant, C. Johnson, F. A. Parpia, and E. Plummer, *Computer Physics Communications* **55**, 425 (1989).
- [10] I. P. Grant, *Relativistic Quantum Theory of Atoms and Molecules*, edited by I. P. Grant, Springer Series on Atomic, Optical, and Plasma Physics, Vol. 40 (Springer, New York, NY, 2007).
- [11] B. J. McKenzie, I. P. Grant, and P. H. Norrington, *Computer Physics Communications* **21**, 233 (1980).
- [12] P. J. Mohr, *Physical Review A* **46**, 4421 (1992).
- [13] L. W. Fullerton and G. A. Rinker, *Physical Review A* **13**, 1283 (1976).
- [14] C. Froese Fischer, *Atoms* **2**, 1 (2014).
- [15] C. Froese Fischer, M. R. Godefroid, T. Brage, P. Jönsson, and G. Gaigalas, *Journal of Physics B: Atomic, Molecular and Optical Physics* **49**, 182004 (2016).
- [16] A. E. Kramida, *Fusion Science and Technology* **63**, 313 (2013).
- [17] M. F. Gu, *Canadian Journal of Physics* **86**, 675 (2008).
- [18] N. Kimura and N. Nakamura, *Journal of Physics B: Atomic, Molecular and Optical Physics* **56**, 225001 (2023)

Explanation of Tables

Tables 1-5.

J	Total momentum of the state
p	Parity of the state
E	Energy of atomic level relative to the groundstate (cm^{-1}/eV)

Tables 6-10.

λ	Transition wavelength (nm)
A	Transition rate for magnetic-type transitions (s^{-1})

Only transitions with $A > 10 \text{ s}^{-1}$ are listed.

Table 1I⁸⁺ levels, 4d⁹ valence electronic configuration (Rh-like ion).

No.	<i>J</i>	<i>p</i>	LS-composition	<i>E</i> (cm ⁻¹)	<i>E</i> (eV)
1	5/2	+	0.96 3d ¹⁰ (₀ ¹ S) 4s ² 4p ⁶ 4d ⁹ ² D	0	0.0000
2	3/2	+	0.96 3d ¹⁰ (₀ ¹ S) 4s ² 4p ⁶ 4d ⁹ ² D	14383	1.7832

Table 2I⁹⁺ levels, 4d⁸ valence electronic configuration (Ru-like ion).

No.	<i>J</i>	<i>p</i>	LS-composition	<i>E</i> (cm ⁻¹)	<i>E</i> (eV)
1	4	+	0.94 3d ¹⁰ (₀ ¹ S) 4s ² 4p ⁶ 4d ⁸ (₂ ³ F) ³ F + 0.02 3d ¹⁰ (₀ ¹ S) 4s ² 4p ⁶ 4d ⁸ (₂ ¹ G) ¹ G	0	0.0000
2	2	+	0.40 3d ¹⁰ (₀ ¹ S) 4s ² 4p ⁶ 4d ⁸ (₂ ¹ D) ¹ D + 0.38 3d ¹⁰ (₀ ¹ S) 4s ² 4p ⁶ 4d ⁸ (₂ ³ F) ³ F + 0.18 3d ¹⁰ (₀ ¹ S) 4s ² 4p ⁶ 4d ⁸ (₂ ³ P) ³ P	12506	1.5505
3	3	+	0.96 3d ¹⁰ (₀ ¹ S) 4s ² 4p ⁶ 4d ⁸ (₂ ³ F) ³ F	13052	1.6182
4	2	+	0.53 3d ¹⁰ (₀ ¹ S) 4s ² 4p ⁶ 4d ⁸ (₂ ³ P) ³ P + 0.41 3d ¹⁰ (₀ ¹ S) 4s ² 4p ⁶ 4d ⁸ (₂ ³ F) ³ F	24030	2.9793
5	0	+	0.88 3d ¹⁰ (₀ ¹ S) 4s ² 4p ⁶ 4d ⁸ (₂ ³ P) ³ P + 0.08 3d ¹⁰ (₀ ¹ S) 4s ² 4p ⁶ 4d ⁸ (₀ ¹ S) ¹ S	30639	3.7987
6	1	+	0.96 3d ¹⁰ (₀ ¹ S) 4s ² 4p ⁶ 4d ⁸ (₂ ³ P) ³ P	31968	3.9635
7	4	+	0.94 3d ¹⁰ (₀ ¹ S) 4s ² 4p ⁶ 4d ⁸ (₂ ¹ G) ¹ G + 0.02 3d ¹⁰ (₀ ¹ S) 4s ² 4p ⁶ 4d ⁸ (₂ ³ F) ³ F	38430	4.7647
8	2	+	0.54 3d ¹⁰ (₀ ¹ S) 4s ² 4p ⁶ 4d ⁸ (₂ ¹ D) ¹ D + 0.25 3d ¹⁰ (₀ ¹ S) 4s ² 4p ⁶ 4d ⁸ (₂ ³ P) ³ P + 0.17 3d ¹⁰ (₀ ¹ S) 4s ² 4p ⁶ 4d ⁸ (₂ ³ F) ³ F	38488	4.7719
9	0	+	0.87 3d ¹⁰ (₀ ¹ S) 4s ² 4p ⁶ 4d ⁸ (₀ ¹ S) ¹ S + 0.08 3d ¹⁰ (₀ ¹ S) 4s ² 4p ⁶ 4d ⁸ (₂ ³ P) ³ P	83632	10.3691

Table 3I¹⁰⁺ levels, 4d⁷ valence electronic configuration (Tc-like ion).

No.	J	p	LS-composition	E (cm ⁻¹)	E (eV)
1	9/2	+	0.87 3d ¹⁰ (¹ S) 4s ² 4p ⁶ 4d ⁷ (⁴ F) ⁴ F + 0.09 3d ¹⁰ (¹ S) 4s ² 4p ⁶ 4d ⁷ (² G) ² G	0	0.0000
2	7/2	+	0.94 3d ¹⁰ (¹ S) 4s ² 4p ⁶ 4d ⁷ (⁴ F) ⁴ F + 0.02 3d ¹⁰ (¹ S) 4s ² 4p ⁶ 4d ⁷ (² G) ² G	11708	1.4516
3	5/2	+	0.79 3d ¹⁰ (¹ S) 4s ² 4p ⁶ 4d ⁷ (⁴ F) ⁴ F + 0.08 3d ¹⁰ (¹ S) 4s ² 4p ⁶ 4d ⁷ (² D) ² D + 0.05 3d ¹⁰ (¹ S) 4s ² 4p ⁶ 4d ⁷ (² D) ² D	16052	1.9902
4	3/2	+	0.51 3d ¹⁰ (¹ S) 4s ² 4p ⁶ 4d ⁷ (⁴ F) ⁴ F + 0.19 3d ¹⁰ (¹ S) 4s ² 4p ⁶ 4d ⁷ (² P) ² P + 0.16 3d ¹⁰ (¹ S) 4s ² 4p ⁶ 4d ⁷ (² D) ² D	17576	2.1791
5	3/2	+	0.41 3d ¹⁰ (¹ S) 4s ² 4p ⁶ 4d ⁷ (⁴ P) ⁴ P + 0.29 3d ¹⁰ (¹ S) 4s ² 4p ⁶ 4d ⁷ (⁴ F) ⁴ F + 0.26 3d ¹⁰ (¹ S) 4s ² 4p ⁶ 4d ⁷ (² P) ² P	23999	2.9755
6	5/2	+	0.86 3d ¹⁰ (¹ S) 4s ² 4p ⁶ 4d ⁷ (⁴ P) ⁴ P + 0.06 3d ¹⁰ (¹ S) 4s ² 4p ⁶ 4d ⁷ (⁴ F) ⁴ F + 0.03 3d ¹⁰ (¹ S) 4s ² 4p ⁶ 4d ⁷ (² D) ² D	27006	3.3483
7	9/2	+	0.64 3d ¹⁰ (¹ S) 4s ² 4p ⁶ 4d ⁷ (² G) ² G + 0.23 3d ¹⁰ (¹ S) 4s ² 4p ⁶ 4d ⁷ (² H) ² H + 0.09 3d ¹⁰ (¹ S) 4s ² 4p ⁶ 4d ⁷ (⁴ F) ⁴ F	30024	3.7225
8	1/2	+	0.69 3d ¹⁰ (¹ S) 4s ² 4p ⁶ 4d ⁷ (⁴ P) ⁴ P + 0.27 3d ¹⁰ (¹ S) 4s ² 4p ⁶ 4d ⁷ (² P) ² P	32539	4.0344
9	7/2	+	0.88 3d ¹⁰ (¹ S) 4s ² 4p ⁶ 4d ⁷ (² G) ² G + 0.07 3d ¹⁰ (¹ S) 4s ² 4p ⁶ 4d ⁷ (² F) ² F	39893	4.9461
10	11/2	+	0.96 3d ¹⁰ (¹ S) 4s ² 4p ⁶ 4d ⁷ (² H) ² H	40353	5.0032
11	3/2	+	0.41 3d ¹⁰ (¹ S) 4s ² 4p ⁶ 4d ⁷ (⁴ P) ⁴ P + 0.24 3d ¹⁰ (¹ S) 4s ² 4p ⁶ 4d ⁷ (² P) ² P + 0.18 3d ¹⁰ (¹ S) 4s ² 4p ⁶ 4d ⁷ (² D) ² D	42753	5.3007
12	5/2	+	0.61 3d ¹⁰ (¹ S) 4s ² 4p ⁶ 4d ⁷ (² D) ² D + 0.18 3d ¹⁰ (¹ S) 4s ² 4p ⁶ 4d ⁷ (² D) ² D + 0.10 3d ¹⁰ (¹ S) 4s ² 4p ⁶ 4d ⁷ (⁴ F) ⁴ F	45583	5.6516
13	1/2	+	0.69 3d ¹⁰ (¹ S) 4s ² 4p ⁶ 4d ⁷ (² P) ² P + 0.27 3d ¹⁰ (¹ S) 4s ² 4p ⁶ 4d ⁷ (⁴ P) ⁴ P	49927	6.1902
14	9/2	+	0.73 3d ¹⁰ (¹ S) 4s ² 4p ⁶ 4d ⁷ (² H) ² H + 0.23 3d ¹⁰ (¹ S) 4s ² 4p ⁶ 4d ⁷ (² G) ² G	52753	6.5405
15	5/2	+	0.88 3d ¹⁰ (¹ S) 4s ² 4p ⁶ 4d ⁷ (² F) ² F + 0.05 3d ¹⁰ (¹ S) 4s ² 4p ⁶ 4d ⁷ (² D) ² D	58169	7.2121
16	3/2	+	0.57 3d ¹⁰ (¹ S) 4s ² 4p ⁶ 4d ⁷ (² D) ² D + 0.27 3d ¹⁰ (¹ S) 4s ² 4p ⁶ 4d ⁷ (² P) ² P + 0.06 3d ¹⁰ (¹ S) 4s ² 4p ⁶ 4d ⁷ (⁴ P) ⁴ P	62197	7.7114
17	7/2	+	0.89 3d ¹⁰ (¹ S) 4s ² 4p ⁶ 4d ⁷ (² F) ² F + 0.06 3d ¹⁰ (¹ S) 4s ² 4p ⁶ 4d ⁷ (² G) ² G	65442	8.1137
18	3/2	+	0.89 3d ¹⁰ (¹ S) 4s ² 4p ⁶ 4d ⁷ (² D) ² D + 0.05 3d ¹⁰ (¹ S) 4s ² 4p ⁶ 4d ⁷ (² D) ² D	92481	11.4662
19	5/2	+	0.68 3d ¹⁰ (¹ S) 4s ² 4p ⁶ 4d ⁷ (² D) ² D + 0.21 3d ¹⁰ (¹ S) 4s ² 4p ⁶ 4d ⁷ (² D) ² D + 0.06 3d ¹⁰ (¹ S) 4s ² 4p ⁶ 4d ⁷ (² F) ² F	97525	12.0916

Table 4I¹¹⁺ levels, 4d⁶ valence electronic configuration (Mo-like ion).

No.	<i>J</i>	<i>p</i>	LS-composition			<i>E</i> (cm ⁻¹)	<i>E</i> (eV)
1	4	+	0.86 $3d^{10}(^1S)4s^24p^64d^6(^5D)$ 5D + 0.06 $3d^{10}(^1S)4s^24p^64d^6(^3F)$ 3F + 0.04 $3d^{10}(^1S)4s^24p^64d^6(^3F)$ 3F			0	0.0000
2	3	+	0.91 $3d^{10}(^1S)4s^24p^64d^6(^5D)$ 5D + 0.02 $3d^{10}(^1S)4s^24p^64d^6(^3F)$ 3F			8593	1.0654
3	2	+	0.74 $3d^{10}(^1S)4s^24p^64d^6(^5D)$ 5D + 0.09 $3d^{10}(^1S)4s^24p^64d^6(^3P)$ 3P + 0.08 $3d^{10}(^1S)4s^24p^64d^6(^3P)$ 3P			9788	1.2136
4	1	+	0.85 $3d^{10}(^1S)4s^24p^64d^6(^5D)$ 5D + 0.06 $3d^{10}(^1S)4s^24p^64d^6(^3P)$ 3P + 0.04 $3d^{10}(^1S)4s^24p^64d^6(^3P)$ 3P			13920	1.7259
5	0	+	0.83 $3d^{10}(^1S)4s^24p^64d^6(^5D)$ 5D + 0.08 $3d^{10}(^1S)4s^24p^64d^6(^3P)$ 3P + 0.03 $3d^{10}(^1S)4s^24p^64d^6(^3P)$ 3P			14988	1.8582
6	4	+	0.26 $3d^{10}(^1S)4s^24p^64d^6(^3H)$ 3H + 0.24 $3d^{10}(^1S)4s^24p^64d^6(^3G)$ 3G + 0.15 $3d^{10}(^1S)4s^24p^64d^6(^3F)$ 3F			29831	3.6985
7	2	+	0.40 $3d^{10}(^1S)4s^24p^64d^6(^3P)$ 3P + 0.21 $3d^{10}(^1S)4s^24p^64d^6(^5D)$ 5D + 0.20 $3d^{10}(^1S)4s^24p^64d^6(^3P)$ 3P			34613	4.2915
8	5	+	0.54 $3d^{10}(^1S)4s^24p^64d^6(^3H)$ 3H + 0.43 $3d^{10}(^1S)4s^24p^64d^6(^3G)$ 3G			35459	4.3964
9	6	+	0.85 $3d^{10}(^1S)4s^24p^64d^6(^3H)$ 3H + 0.11 $3d^{10}(^1S)4s^24p^64d^6(^1I)$ 1I			35605	4.4144
10	3	+	0.44 $3d^{10}(^1S)4s^24p^64d^6(^3F)$ 3F + 0.31 $3d^{10}(^1S)4s^24p^64d^6(^3G)$ 3G + 0.14 $3d^{10}(^1S)4s^24p^64d^6(^3F)$ 3F			40865	5.0667
11	2	+	0.71 $3d^{10}(^1S)4s^24p^64d^6(^3F)$ 3F + 0.11 $3d^{10}(^1S)4s^24p^64d^6(^1D)$ 1D + 0.06 $3d^{10}(^1S)4s^24p^64d^6(^3F)$ 3F			42147	5.2255
12	4	+	0.54 $3d^{10}(^1S)4s^24p^64d^6(^3H)$ 3H + 0.28 $3d^{10}(^1S)4s^24p^64d^6(^3F)$ 3F + 0.10 $3d^{10}(^1S)4s^24p^64d^6(^3F)$ 3F			45975	5.7002
13	0	+	0.37 $3d^{10}(^1S)4s^24p^64d^6(^1S)$ 1S + 0.22 $3d^{10}(^1S)4s^24p^64d^6(^3P)$ 3P + 0.16 $3d^{10}(^1S)4s^24p^64d^6(^3P)$ 3P			50419	6.2512
14	5	+	0.53 $3d^{10}(^1S)4s^24p^64d^6(^3G)$ 3G + 0.43 $3d^{10}(^1S)4s^24p^64d^6(^3H)$ 3H			51332	6.3644
15	1	+	0.52 $3d^{10}(^1S)4s^24p^64d^6(^3D)$ 3D + 0.34 $3d^{10}(^1S)4s^24p^64d^6(^3P)$ 3P + 0.08 $3d^{10}(^1S)4s^24p^64d^6(^5D)$ 5D			51518	6.3874
16	4	+	0.65 $3d^{10}(^1S)4s^24p^64d^6(^3G)$ 3G + 0.13 $3d^{10}(^1S)4s^24p^64d^6(^3F)$ 3F + 0.12 $3d^{10}(^1S)4s^24p^64d^6(^1G)$ 1G			52619	6.5239
17	2	+	0.70 $3d^{10}(^1S)4s^24p^64d^6(^3D)$ 3D + 0.09 $3d^{10}(^1S)4s^24p^64d^6(^3P)$ 3P + 0.06 $3d^{10}(^1S)4s^24p^64d^6(^3F)$ 3F			54384	6.7428
18	3	+	0.41 $3d^{10}(^1S)4s^24p^64d^6(^3G)$ 3G + 0.37 $3d^{10}(^1S)4s^24p^64d^6(^3F)$ 3F + 0.10 $3d^{10}(^1S)4s^24p^64d^6(^3D)$ 3D			55886	6.9289

No.	<i>J</i>	<i>p</i>	LS-composition				<i>E</i> (cm ⁻¹)	<i>E</i> (eV)
19	3	+	0.73 $3d^{10}(^1S)4s^24p^64d^6(^3D)$ 3D + 0.20 $3d^{10}(^1S)4s^24p^64d^6(^3G)$ 3G +				56957	7.0617
			0.02 $3d^{10}(^1S)4s^24p^64d^6(^3F)$ 3F					
20	6	+	0.85 $3d^{10}(^1S)4s^24p^64d^6(^4I)$ 1I + 0.11 $3d^{10}(^1S)4s^24p^64d^6(^3H)$ 3H				60399	7.4885
21	1	+	0.41 $3d^{10}(^1S)4s^24p^64d^6(^3D)$ 3D + 0.35 $3d^{10}(^1S)4s^24p^64d^6(^3P)$ 3P +				60946	7.5563
			0.17 $3d^{10}(^1S)4s^24p^64d^6(^3P)$ 3P					
22	0	+	0.67 $3d^{10}(^1S)4s^24p^64d^6(^3P)$ 3P + 0.19 $3d^{10}(^1S)4s^24p^64d^6(^3P)$ 3P +				67808	8.4072
			0.05 $3d^{10}(^1S)4s^24p^64d^6(^1S)$ 1S					
23	4	+	0.59 $3d^{10}(^1S)4s^24p^64d^6(^1G)$ 1G + 0.16 $3d^{10}(^1S)4s^24p^64d^6(^3F)$ 3F +				68988	8.5534
			0.12 $3d^{10}(^1S)4s^24p^64d^6(^3H)$ 3H					
24	3	+	0.66 $3d^{10}(^1S)4s^24p^64d^6(^1F)$ 1F + 0.23 $3d^{10}(^1S)4s^24p^64d^6(^3F)$ 3F +				70632	8.7573
			0.05 $3d^{10}(^1S)4s^24p^64d^6(^3F)$ 3F					
25	2	+	0.54 $3d^{10}(^1S)4s^24p^64d^6(^1D)$ 1D + 0.12 $3d^{10}(^1S)4s^24p^64d^6(^3F)$ 3F +				71747	8.8955
			0.09 $3d^{10}(^1S)4s^24p^64d^6(^1D)$ 1D					
26	1	+	0.70 $3d^{10}(^1S)4s^24p^64d^6(^3P)$ 3P + 0.22 $3d^{10}(^1S)4s^24p^64d^6(^3P)$ 3P				82643	10.2464
27	4	+	0.70 $3d^{10}(^1S)4s^24p^64d^6(^3F)$ 3F + 0.13 $3d^{10}(^1S)4s^24p^64d^6(^3F)$ 3F +				88256	10.9424
			0.08 $3d^{10}(^1S)4s^24p^64d^6(^1G)$ 1G					
28	2	+	0.81 $3d^{10}(^1S)4s^24p^64d^6(^3F)$ 3F + 0.09 $3d^{10}(^1S)4s^24p^64d^6(^3F)$ 3F +				89378	11.0815
			0.04 $3d^{10}(^1S)4s^24p^64d^6(^3D)$ 3D					
29	0	+	0.51 $3d^{10}(^1S)4s^24p^64d^6(^3P)$ 3P + 0.37 $3d^{10}(^1S)4s^24p^64d^6(^1S)$ 1S +				90368	11.2042
			0.03 $3d^{10}(^1S)4s^24p^64d^6(^3P)$ 3P					
30	2	+	0.52 $3d^{10}(^1S)4s^24p^64d^6(^3P)$ 3P + 0.29 $3d^{10}(^1S)4s^24p^64d^6(^3P)$ 3P +				97150	12.0451
			0.06 $3d^{10}(^1S)4s^24p^64d^6(^1D)$ 1D					
31	3	+	0.56 $3d^{10}(^1S)4s^24p^64d^6(^3F)$ 3F + 0.22 $3d^{10}(^1S)4s^24p^64d^6(^1F)$ 1F +				97262	12.0590
			0.08 $3d^{10}(^1S)4s^24p^64d^6(^3F)$ 3F					
32	4	+	0.61 $3d^{10}(^1S)4s^24p^64d^6(^1G)$ 1G + 0.22 $3d^{10}(^1S)4s^24p^64d^6(^1G)$ 1G +				102037	12.6510
			0.06 $3d^{10}(^1S)4s^24p^64d^6(^3F)$ 3F					
33	2	+	0.76 $3d^{10}(^1S)4s^24p^64d^6(^1D)$ 1D + 0.18 $3d^{10}(^1S)4s^24p^64d^6(^1D)$ 1D				127612	15.8219
34	0	+	0.77 $3d^{10}(^1S)4s^24p^64d^6(^1S)$ 1S + 0.16 $3d^{10}(^1S)4s^24p^64d^6(^1S)$ 1S +				164497	20.3950
			0.02 $3d^{10}(^1S)4s^24p^64d^6(^3P)$ 3P					

Table 5I¹²⁺ levels, 4d⁵ valence electronic configuration (Nb-like ion).

No.	J	p	LS-composition	E (cm ⁻¹)	E (eV)
1	5/2	+	0.88 3d ¹⁰ (₀ S) 4s ² 4p ⁶ 4d ⁵ (₅ S) 6S + 0.08 3d ¹⁰ (₀ S) 4s ² 4p ⁶ 4d ⁵ (₃ P) 4P	0	0.0000
2	5/2	+	0.34 3d ¹⁰ (₀ S) 4s ² 4p ⁶ 4d ⁵ (₅ G) 4G + 0.15 3d ¹⁰ (₀ S) 4s ² 4p ⁶ 4d ⁵ (₃ F) 2F + 0.15 3d ¹⁰ (₀ S) 4s ² 4p ⁶ 4d ⁵ (₅ D) 4D	37613	4.6634
3	7/2	+	0.72 3d ¹⁰ (₀ S) 4s ² 4p ⁶ 4d ⁵ (₅ G) 4G + 0.09 3d ¹⁰ (₀ S) 4s ² 4p ⁶ 4d ⁵ (₅ D) 4D + 0.09 3d ¹⁰ (₀ S) 4s ² 4p ⁶ 4d ⁵ (₃ F) 2F	44372	5.5014
4	11/2	+	0.84 3d ¹⁰ (₀ S) 4s ² 4p ⁶ 4d ⁵ (₅ G) 4G + 0.10 3d ¹⁰ (₀ S) 4s ² 4p ⁶ 4d ⁵ (₃ H) 2H + 0.02 3d ¹⁰ (₀ S) 4s ² 4p ⁶ 4d ⁵ (₅ I) 2I	46119	5.7180
5	5/2	+	0.43 3d ¹⁰ (₀ S) 4s ² 4p ⁶ 4d ⁵ (₅ G) 4G + 0.23 3d ¹⁰ (₀ S) 4s ² 4p ⁶ 4d ⁵ (₅ D) 4D + 0.21 3d ¹⁰ (₀ S) 4s ² 4p ⁶ 4d ⁵ (₃ P) 4P	46333	5.7445
6	3/2	+	0.45 3d ¹⁰ (₀ S) 4s ² 4p ⁶ 4d ⁵ (₃ P) 4P + 0.44 3d ¹⁰ (₀ S) 4s ² 4p ⁶ 4d ⁵ (₅ D) 4D + 0.03 3d ¹⁰ (₀ S) 4s ² 4p ⁶ 4d ⁵ (₃ F) 4F	46461	5.7605
7	9/2	+	0.87 3d ¹⁰ (₀ S) 4s ² 4p ⁶ 4d ⁵ (₅ G) 4G + 0.05 3d ¹⁰ (₀ S) 4s ² 4p ⁶ 4d ⁵ (₃ F) 4F + 0.03 3d ¹⁰ (₀ S) 4s ² 4p ⁶ 4d ⁵ (₃ H) 2H	47255	5.8589
8	1/2	+	0.61 3d ¹⁰ (₀ S) 4s ² 4p ⁶ 4d ⁵ (₃ P) 4P + 0.32 3d ¹⁰ (₀ S) 4s ² 4p ⁶ 4d ⁵ (₅ D) 4D + 0.04 3d ¹⁰ (₀ S) 4s ² 4p ⁶ 4d ⁵ (₅ S) 2S	51380	6.3703
9	7/2	+	0.73 3d ¹⁰ (₀ S) 4s ² 4p ⁶ 4d ⁵ (₅ D) 4D + 0.16 3d ¹⁰ (₀ S) 4s ² 4p ⁶ 4d ⁵ (₅ G) 4G + 0.06 3d ¹⁰ (₀ S) 4s ² 4p ⁶ 4d ⁵ (₃ F) 4F	55605	6.8941
10	5/2	+	0.40 3d ¹⁰ (₀ S) 4s ² 4p ⁶ 4d ⁵ (₅ D) 4D + 0.19 3d ¹⁰ (₀ S) 4s ² 4p ⁶ 4d ⁵ (₃ P) 4P + 0.17 3d ¹⁰ (₀ S) 4s ² 4p ⁶ 4d ⁵ (₅ D) 2D	60412	7.4902
11	1/2	+	0.64 3d ¹⁰ (₀ S) 4s ² 4p ⁶ 4d ⁵ (₅ D) 4D + 0.30 3d ¹⁰ (₀ S) 4s ² 4p ⁶ 4d ⁵ (₃ P) 4P + 0.02 3d ¹⁰ (₀ S) 4s ² 4p ⁶ 4d ⁵ (₅ S) 2S	62506	7.7497
12	3/2	+	0.44 3d ¹⁰ (₀ S) 4s ² 4p ⁶ 4d ⁵ (₅ D) 4D + 0.44 3d ¹⁰ (₀ S) 4s ² 4p ⁶ 4d ⁵ (₃ P) 4P + 0.04 3d ¹⁰ (₀ S) 4s ² 4p ⁶ 4d ⁵ (₅ D) 2D	64755	8.0286
13	11/2	+	0.75 3d ¹⁰ (₀ S) 4s ² 4p ⁶ 4d ⁵ (₅ I) 2I + 0.14 3d ¹⁰ (₀ S) 4s ² 4p ⁶ 4d ⁵ (₃ H) 2H + 0.08 3d ¹⁰ (₀ S) 4s ² 4p ⁶ 4d ⁵ (₅ G) 4G	66233	8.2118
14	7/2	+	0.33 3d ¹⁰ (₀ S) 4s ² 4p ⁶ 4d ⁵ (₃ F) 4F + 0.22 3d ¹⁰ (₀ S) 4s ² 4p ⁶ 4d ⁵ (₃ F) 2F + 0.20 3d ¹⁰ (₀ S) 4s ² 4p ⁶ 4d ⁵ (₅ F) 2F	70003	8.6793
15	13/2	+	0.97 3d ¹⁰ (₀ S) 4s ² 4p ⁶ 4d ⁵ (₅ I) 2I	71684	8.8876
16	3/2	+	0.47 3d ¹⁰ (₀ S) 4s ² 4p ⁶ 4d ⁵ (₅ F) 4F + 0.30 3d ¹⁰ (₀ S) 4s ² 4p ⁶ 4d ⁵ (₅ D) 2D + 0.13 3d ¹⁰ (₀ S) 4s ² 4p ⁶ 4d ⁵ (₁ D) 2D	72030	8.9306
17	9/2	+	0.43 3d ¹⁰ (₀ S) 4s ² 4p ⁶ 4d ⁵ (₅ G) 2G + 0.37 3d ¹⁰ (₀ S) 4s ² 4p ⁶ 4d ⁵ (₃ F) 4F + 0.08 3d ¹⁰ (₀ S) 4s ² 4p ⁶ 4d ⁵ (₂ H) 2H	72135	8.9435

No.	J	p	LS-composition	E (cm $^{-1}$)	E (eV)
18	5/2	+	0.20 $3d^{10}(^1S) 4s^2 4p^6 4d^5(^4F)$ 4F + 0.19 $3d^{10}(^1S) 4s^2 4p^6 4d^5(^4P)$ 4P + 73357 0.13 $3d^{10}(^1S) 4s^2 4p^6 4d^5(^2F)$ 2F	73357	9.0951
19	5/2	+	0.41 $3d^{10}(^1S) 4s^2 4p^6 4d^5(^4F)$ 4F + 0.22 $3d^{10}(^1S) 4s^2 4p^6 4d^5(^2F)$ 2F + 79823 0.11 $3d^{10}(^1S) 4s^2 4p^6 4d^5(^4D)$ 4D	79823	9.8968
20	9/2	+	0.50 $3d^{10}(^1S) 4s^2 4p^6 4d^5(^2H)$ 2H + 0.39 $3d^{10}(^1S) 4s^2 4p^6 4d^5(^4F)$ 4F + 83044 0.07 $3d^{10}(^1S) 4s^2 4p^6 4d^5(^2G)$ 2G	83044	10.2962
21	7/2	+	0.49 $3d^{10}(^1S) 4s^2 4p^6 4d^5(^2G)$ 2G + 0.18 $3d^{10}(^1S) 4s^2 4p^6 4d^5(^2F)$ 2F + 84872 0.15 $3d^{10}(^1S) 4s^2 4p^6 4d^5(^4F)$ 4F	84872	10.5228
22	3/2	+	0.43 $3d^{10}(^1S) 4s^2 4p^6 4d^5(^2D)$ 2D + 0.42 $3d^{10}(^1S) 4s^2 4p^6 4d^5(^4F)$ 4F + 87237 0.04 $3d^{10}(^1S) 4s^2 4p^6 4d^5(^2D)$ 2D	87237	10.8160
23	5/2	+	0.57 $3d^{10}(^1S) 4s^2 4p^6 4d^5(^2F)$ 2F + 0.18 $3d^{10}(^1S) 4s^2 4p^6 4d^5(^4F)$ 4F + 89208 0.11 $3d^{10}(^1S) 4s^2 4p^6 4d^5(^2D)$ 2D	89208	11.0604
24	7/2	+	0.53 $3d^{10}(^1S) 4s^2 4p^6 4d^5(^2F)$ 2F + 0.23 $3d^{10}(^1S) 4s^2 4p^6 4d^5(^2G)$ 2G + 89254 0.07 $3d^{10}(^1S) 4s^2 4p^6 4d^5(^4F)$ 4F	89254	11.0661
25	7/2	+	0.50 $3d^{10}(^1S) 4s^2 4p^6 4d^5(^2F)$ 2F + 0.30 $3d^{10}(^1S) 4s^2 4p^6 4d^5(^4F)$ 4F + 94894 0.08 $3d^{10}(^1S) 4s^2 4p^6 4d^5(^2G)$ 2G	94894	11.7653
26	11/2	+	0.73 $3d^{10}(^1S) 4s^2 4p^6 4d^5(^2H)$ 2H + 0.19 $3d^{10}(^1S) 4s^2 4p^6 4d^5(^2I)$ 2I + 95688 0.05 $3d^{10}(^1S) 4s^2 4p^6 4d^5(^4G)$ 4G	95688	11.8638
27	9/2	+	0.42 $3d^{10}(^1S) 4s^2 4p^6 4d^5(^2G)$ 2G + 0.35 $3d^{10}(^1S) 4s^2 4p^6 4d^5(^2H)$ 2H + 96867 0.15 $3d^{10}(^1S) 4s^2 4p^6 4d^5(^4F)$ 4F	96867	12.0100
28	1/2	+	0.85 $3d^{10}(^1S) 4s^2 4p^6 4d^5(^2S)$ 2S + 0.06 $3d^{10}(^1S) 4s^2 4p^6 4d^5(^4P)$ 4P + 97669 0.05 $3d^{10}(^1S) 4s^2 4p^6 4d^5(^2P)$ 2P	97669	12.1095
29	5/2	+	0.37 $3d^{10}(^1S) 4s^2 4p^6 4d^5(^2F)$ 2F + 0.31 $3d^{10}(^1S) 4s^2 4p^6 4d^5(^2D)$ 2D + 102865 0.09 $3d^{10}(^1S) 4s^2 4p^6 4d^5(^2D)$ 2D	102865	12.7537
30	3/2	+	0.86 $3d^{10}(^1S) 4s^2 4p^6 4d^5(^2D)$ 2D + 0.04 $3d^{10}(^1S) 4s^2 4p^6 4d^5(^2D)$ 2D + 109658 0.04 $3d^{10}(^1S) 4s^2 4p^6 4d^5(^4D)$ 4D	109658	13.5958
31	5/2	+	0.69 $3d^{10}(^1S) 4s^2 4p^6 4d^5(^2D)$ 2D + 0.15 $3d^{10}(^1S) 4s^2 4p^6 4d^5(^2F)$ 2F + 115818 0.05 $3d^{10}(^1S) 4s^2 4p^6 4d^5(^4D)$ 4D	115818	14.3596
32	9/2	+	0.92 $3d^{10}(^1S) 4s^2 4p^6 4d^5(^2G)$ 2G + 0.03 $3d^{10}(^1S) 4s^2 4p^6 4d^5(^2G)$ 2G 121622 15.0792	121622	15.0792
33	7/2	+	0.84 $3d^{10}(^1S) 4s^2 4p^6 4d^5(^2G)$ 2G + 0.07 $3d^{10}(^1S) 4s^2 4p^6 4d^5(^2F)$ 2F + 124367 0.04 $3d^{10}(^1S) 4s^2 4p^6 4d^5(^2G)$ 2G	124367	15.4196
34	3/2	+	0.84 $3d^{10}(^1S) 4s^2 4p^6 4d^5(^2P)$ 2P + 0.08 $3d^{10}(^1S) 4s^2 4p^6 4d^5(^2D)$ 2D + 140213 0.03 $3d^{10}(^1S) 4s^2 4p^6 4d^5(^2D)$ 2D	140213	17.3842
35	1/2	+	0.90 $3d^{10}(^1S) 4s^2 4p^6 4d^5(^2P)$ 2P + 0.05 $3d^{10}(^1S) 4s^2 4p^6 4d^5(^2S)$ 2S 145774 18.0737	145774	18.0737
36	5/2	+	0.76 $3d^{10}(^1S) 4s^2 4p^6 4d^5(^2D)$ 2D + 0.16 $3d^{10}(^1S) 4s^2 4p^6 4d^5(^2D)$ 2D + 158534 0.02 $3d^{10}(^1S) 4s^2 4p^6 4d^5(^2D)$ 2D	158534	19.6558

No.	<i>J</i>	<i>p</i>	LS-composition				<i>E</i> (cm ⁻¹)	<i>E</i> (eV)
37	3/2	+	0.65 $3d^{10}(^1_0S)4s^24p^64d^5(^2_1D)$ 2D + 0.15 $3d^{10}(^1_0S)4s^24p^64d^5(^2_5D)$ 2D + 0.12 $3d^{10}(^1_0S)4s^24p^64d^5(^2_3P)$ 2P				162282	20.1204

Table 6M1 transition for I⁸⁺ ion.

Upper level No.	Upper level No.	λ (nm)	A (s ⁻¹)
2	1	695.29	48.09

Table 7Selected M1 transitions for I⁹⁺ ion.

Upper level No.	Upper level No.	λ (nm)	A (s ⁻¹)
9	6	193.56	6.37×10^2
7	1	260.21	4.67×10^1
8	3	393.14	1.05×10^2
6	2	513.82	3.02×10^1
8	4	691.66	3.88×10^1
3	1	766.17	5.63×10^1
4	2	867.74	2.17×10^1
4	3	910.90	2.01×10^1

Table 8Selected M1 transitions for I¹⁰⁺ ion.

Upper level No.	Upper level No.	λ (nm)	A (s^{-1})
19	2	116.53	1.84×10^1
18	3	130.84	1.01×10^1
18	4	133.50	4.48×10^1
19	5	136.01	1.39×10^1
19	6	141.81	1.62×10^2
18	6	152.73	6.12×10^1
17	1	152.81	1.17×10^1
19	9	173.51	1.40×10^1
19	11	182.58	4.16×10^1
17	2	186.10	2.35×10^1
19	12	192.52	1.25×10^1
18	11	201.09	8.69×10^1
18	12	213.23	1.77×10^2
16	3	216.71	8.46×10^1
18	13	234.99	1.24×10^1
15	3	237.43	1.35×10^1
15	4	246.34	1.55×10^1
9	1	250.67	1.01×10^1
19	15	254.09	9.58×10^1
16	5	261.80	1.19×10^1
17	7	282.34	4.24×10^1
19	16	283.06	2.76×10^1
18	15	291.44	2.68×10^1
12	2	295.20	2.23×10^2
13	4	309.11	1.10×10^1
19	17	311.69	2.69×10^1
7	1	333.07	8.97×10^1
9	2	354.80	2.44×10^1
11	3	374.52	2.85×10^1
17	9	391.41	2.63×10^1
9	3	419.45	1.12×10^1
14	7	439.96	6.68×10^1
12	5	463.31	2.89×10^1

Upper level No.	Upper level No.	λ (nm)	A (s^{-1})
16	11	514.31	7.72×10^1
11	5	533.22	7.33×10^1
12	6	538.30	1.84×10^1
13	8	575.12	8.59×10^1
16	12	601.91	5.75×10^1
11	6	635.04	6.23×10^1
6	2	653.68	1.34×10^1
8	4	668.28	2.28×10^1
14	10	806.48	2.12×10^1
2	1	854.11	5.06×10^1
9	7	1013.23	1.02×10^1
8	5	1170.93	1.48×10^1
5	3	1258.37	1.08×10^1

Table 9Selected M1 transitions for I¹¹⁺ ion.

Upper level No.	Upper level No.	λ (nm)	A (s ⁻¹)
34	21	96.57	9.75×10^1
33	7	107.53	1.30×10^1
31	2	112.78	2.18×10^1
30	2	112.92	8.37×10^1
27	1	113.31	2.65×10^1
31	3	114.32	1.02×10^1
33	10	115.28	1.44×10^1
34	26	122.17	7.66×10^2
27	2	125.53	2.07×10^1
28	3	125.64	1.07×10^1
29	4	130.81	1.18×10^2
33	15	131.42	8.75×10^1
26	3	137.26	1.16×10^2
33	18	139.42	2.15×10^1
33	19	141.53	8.57×10^1
26	5	147.81	2.42×10^1
33	21	150.00	1.87×10^1
25	2	158.34	2.31×10^1
30	7	159.91	1.11×10^1
27	6	171.16	2.71×10^1
33	24	175.50	2.08×10^1
19	1	175.57	7.12×10^1
31	10	177.31	1.83×10^1
32	12	178.37	9.65×10^1
31	11	181.44	1.31×10^1
28	7	182.60	1.96×10^1
22	4	185.57	7.32×10^1
27	8	189.41	1.52×10^1
16	1	190.05	1.81×10^1
31	12	194.98	1.90×10^1
21	3	195.47	7.58×10^1
32	14	197.22	8.88×10^1
32	16	202.36	3.24×10^1

Upper level No.	Upper level No.	λ (nm)	A (s^{-1})
28	10	206.13	4.14×10^1
19	2	206.77	1.97×10^1
26	7	208.20	1.74×10^2
18	2	211.45	5.03×10^1
21	4	212.65	4.17×10^1
32	18	216.68	9.09×10^1
12	1	217.51	6.89×10^1
31	16	224.00	2.30×10^1
17	3	224.24	4.13×10^1
27	12	236.51	5.64×10^1
15	3	239.64	1.04×10^1
30	18	242.34	3.29×10^1
10	1	244.71	3.44×10^1
24	6	245.09	2.70×10^1
31	19	248.10	1.72×10^2
30	19	248.80	5.79×10^1
29	15	257.40	3.14×10^2
33	28	261.55	1.20×10^1
28	15	264.13	3.28×10^1
15	4	265.97	2.69×10^1
25	7	269.30	1.75×10^1
27	14	270.83	7.15×10^1
15	5	273.75	7.43×10^1
13	4	273.98	2.83×10^2
30	21	276.21	2.17×10^1
28	17	285.76	7.46×10^1
11	2	298.03	2.19×10^1
23	8	298.25	6.39×10^1
11	3	309.04	4.50×10^1
10	2	309.87	4.95×10^1
26	13	310.33	2.24×10^1
32	24	318.42	2.10×10^1
27	19	319.49	3.15×10^1
26	15	321.28	1.80×10^1
10	3	321.78	1.19×10^1
25	10	323.82	6.06×10^1

Upper level No.	Upper level No.	λ (nm)	A (s^{-1})
6	1	335.23	9.02×10^1
25	11	337.83	6.97×10^1
29	21	339.88	2.99×10^2
28	21	351.71	1.02×10^1
23	10	355.59	3.10×10^1
19	6	368.65	2.99×10^1
21	7	379.76	1.06×10^2
7	2	384.32	2.05×10^2
30	25	393.65	6.98×10^1
20	8	400.97	2.30×10^1
20	9	403.32	5.02×10^1
23	12	434.54	9.09×10^1
19	7	447.56	2.06×10^1
18	7	470.10	1.28×10^1
7	4	483.25	4.37×10^1
25	15	494.33	1.90×10^1
17	7	505.79	1.19×10^1
28	24	533.45	6.16×10^1
23	14	566.39	1.38×10^1
27	24	567.41	2.44×10^1
16	8	582.76	2.41×10^1
15	7	591.56	1.07×10^2
22	15	613.85	4.05×10^1
12	6	619.41	7.37×10^1
19	10	621.46	2.14×10^1
14	8	630.00	2.22×10^1
25	18	630.46	1.37×10^1
14	9	635.83	4.05×10^1
18	10	665.77	1.44×10^1
26	22	674.10	3.62×10^1
30	26	689.32	3.77×10^1
18	11	727.86	2.11×10^1
17	10	739.70	1.01×10^1
10	6	906.23	1.85×10^1
21	15	1060.66	1.03×10^1
31	27	1110.37	1.23×10^1

Upper level No.	Upper level No.	λ (nm)	A (s^{-1})
2	1	1163.71	2.07×10^1

Table 10Selected M1 transitions for I¹²⁺ ion.

Upper level No.	Upper level No.	λ (nm)	A (s^{-1})
36	3	87.59	1.22×10^1
36	5	89.13	2.23×10^1
36	6	89.23	1.64×10^1
37	8	90.17	1.31×10^1
37	10	98.16	4.02×10^1
35	6	100.69	2.31×10^1
36	10	101.91	3.71×10^1
37	12	102.54	3.43×10^1
34	5	106.52	1.94×10^1
37	16	110.80	5.28×10^1
36	14	112.95	2.37×10^1
33	2	115.27	1.01×10^1
36	18	117.40	1.06×10^2
35	11	120.09	2.61×10^1
37	19	121.27	7.27×10^1
35	12	123.43	7.02×10^1
19	1	125.28	3.02×10^1
34	10	125.31	2.28×10^1
36	19	127.05	4.14×10^1
33	5	128.15	1.39×10^1
32	3	129.45	1.26×10^1
32	4	132.45	3.76×10^1
37	22	133.25	2.11×10^1
36	21	135.75	4.41×10^1
18	1	136.32	4.45×10^1
37	23	136.85	1.62×10^2
31	3	139.96	2.36×10^1
31	5	143.91	1.80×10^1
31	6	144.18	4.60×10^1
36	23	144.25	2.31×10^1
36	24	144.34	7.89×10^1
34	16	146.66	2.81×10^1
29	2	153.25	2.82×10^1

Upper level No.	Upper level No.	λ (nm)	A (s^{-1})
12	1	154.43	1.30×10^2
37	28	154.77	1.96×10^1
36	25	157.13	4.47×10^1
30	5	157.92	1.71×10^1
30	6	158.24	2.12×10^1
10	1	165.53	1.23×10^2
34	19	165.59	2.38×10^1
31	9	166.08	1.26×10^2
29	3	170.96	2.03×10^1
30	8	171.59	5.82×10^1
36	29	179.63	1.07×10^1
31	10	180.49	1.09×10^1
33	17	191.45	4.51×10^1
32	14	193.73	5.34×10^1
28	6	195.28	1.63×10^2
31	12	195.84	2.68×10^1
33	18	196.04	1.42×10^1
34	23	196.06	1.46×10^1
26	4	201.74	8.38×10^1
36	30	204.60	1.71×10^2
25	5	205.93	1.37×10^1
26	7	206.47	4.71×10^1
35	28	207.88	2.13×10^2
29	9	211.59	8.13×10^1
30	11	212.08	1.58×10^2
37	31	215.22	1.47×10^2
6	1	215.23	1.70×10^2
5	1	215.83	1.10×10^2
28	8	216.03	4.38×10^1
30	12	222.70	8.78×10^1
24	3	222.80	1.39×10^1
23	3	223.03	4.80×10^1
31	16	228.37	1.64×10^1
23	5	233.23	2.42×10^1
23	6	233.94	1.43×10^1
34	28	235.05	3.14×10^1

Upper level No.	Upper level No.	λ (nm)	A (s^{-1})
24	7	238.10	9.56×10^1
33	20	242.00	2.56×10^1
27	9	242.35	4.27×10^1
33	21	253.20	1.68×10^1
20	3	258.58	4.64×10^1
21	7	265.84	4.64×10^1
2	1	265.87	1.01×10^2
20	4	270.82	3.49×10^1
32	21	272.11	2.43×10^1
30	18	275.48	2.06×10^1
31	19	277.81	4.91×10^1
20	7	279.42	1.02×10^2
18	2	279.76	1.12×10^1
19	3	282.08	4.59×10^1
33	23	284.42	3.77×10^1
16	2	290.55	7.38×10^1
24	9	297.18	9.78×10^1
23	9	297.59	3.72×10^1
19	5	298.60	3.26×10^1
28	12	303.82	4.70×10^1
27	13	326.43	3.30×10^1
30	19	335.18	3.51×10^1
29	18	338.89	1.77×10^2
33	25	339.29	4.82×10^1
26	13	339.50	1.47×10^2
21	9	341.68	2.36×10^1
18	3	345.00	3.42×10^1
24	10	346.72	2.47×10^1
23	10	347.27	1.02×10^1
31	22	349.88	1.07×10^1
17	3	360.19	1.64×10^1
33	27	363.64	3.42×10^1
20	9	364.44	1.23×10^1
12	2	368.43	1.17×10^1
18	5	370.03	2.59×10^2
18	6	371.80	1.39×10^1

Upper level No.	Upper level No.	λ (nm)	A (s^{-1})
22	10	372.79	3.61×10^1
32	25	374.14	3.08×10^1
31	23	375.80	5.90×10^1
31	24	376.45	2.50×10^1
17	4	384.38	2.41×10^1
16	6	391.10	8.60×10^1
25	14	401.76	2.70×10^1
22	11	404.34	2.43×10^1
23	12	408.95	1.05×10^1
19	9	412.91	1.08×10^1
26	15	416.59	3.96×10^1
26	17	424.57	1.97×10^1
29	19	433.98	5.60×10^1
10	2	438.61	1.66×10^1
25	17	439.38	3.68×10^1
14	7	439.60	2.43×10^1
22	12	444.80	4.43×10^1
37	34	453.12	3.46×10^1
31	25	477.91	2.66×10^1
16	8	484.25	1.56×10^1
30	23	489.01	1.05×10^1
13	4	497.17	3.92×10^1
19	10	515.19	5.33×10^1
13	7	526.94	1.01×10^1
12	6	546.64	3.97×10^1
29	21	555.77	1.29×10^1
18	9	563.30	1.50×10^1
23	16	582.15	3.44×10^1
24	17	584.13	3.61×10^1
17	9	604.96	1.23×10^1
11	6	623.28	2.48×10^1
10	3	623.42	2.10×10^1
24	18	629.06	2.04×10^1
23	18	630.88	1.11×10^1
29	22	639.87	2.81×10^1
22	16	657.60	1.62×10^1

Upper level No.	Upper level No.	λ (nm)	A (s^{-1})
25	19	663.53	1.51×10^1
21	14	672.54	1.74×10^1
27	20	723.42	3.61×10^1
29	24	734.69	1.89×10^1
27	21	833.66	1.11×10^1
9	3	890.24	1.17×10^1
11	8	898.82	4.24×10^1
20	17	916.63	1.47×10^1
19	14	1018.37	2.05×10^1
9	5	1078.52	1.22×10^1
6	2	1130.13	1.01×10^1
5	2	1146.81	2.41×10^1

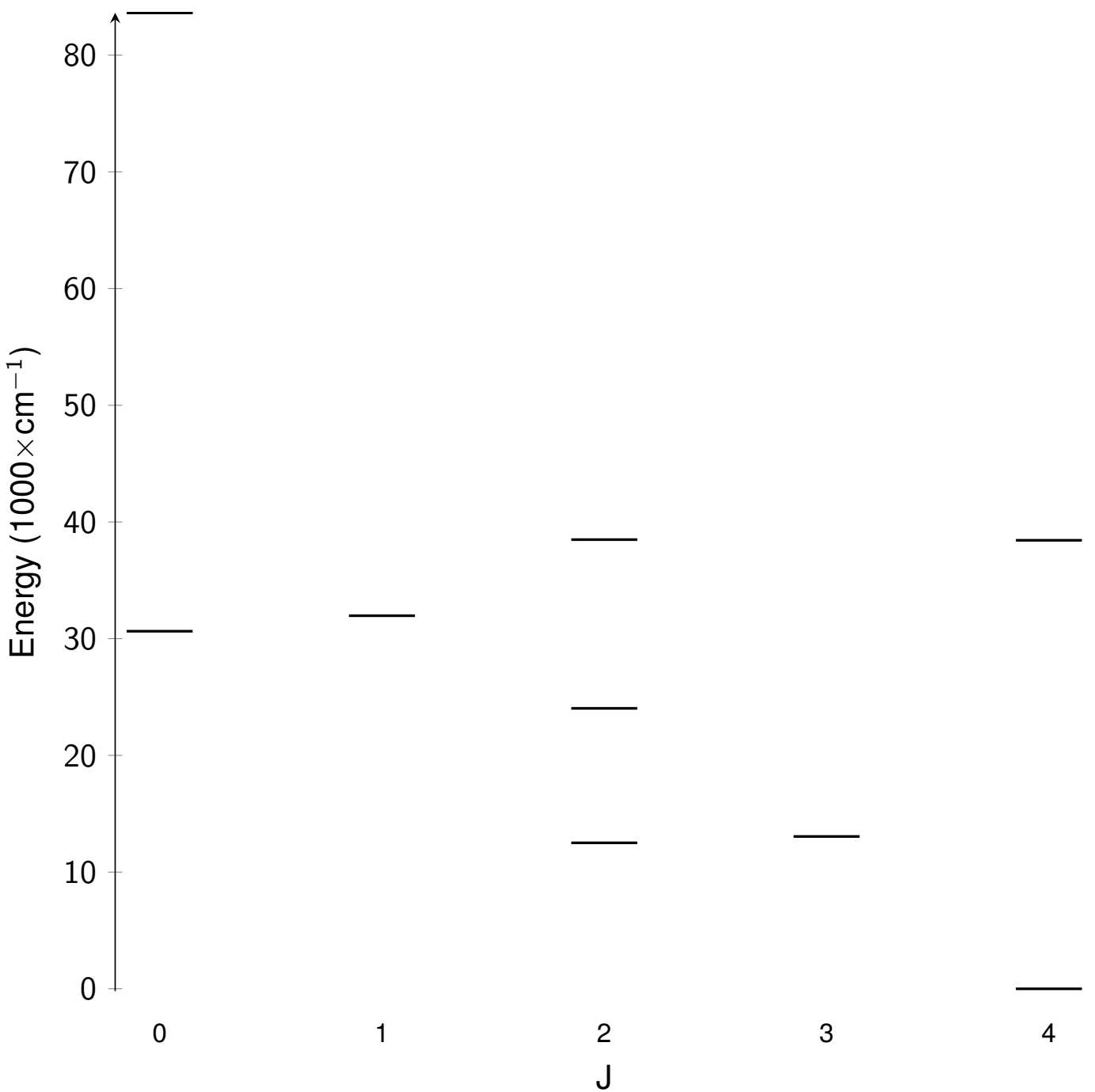


Fig. 6: Energy level diagram for all states of $[Kr]4d^8$ configuration of I^{9+} .

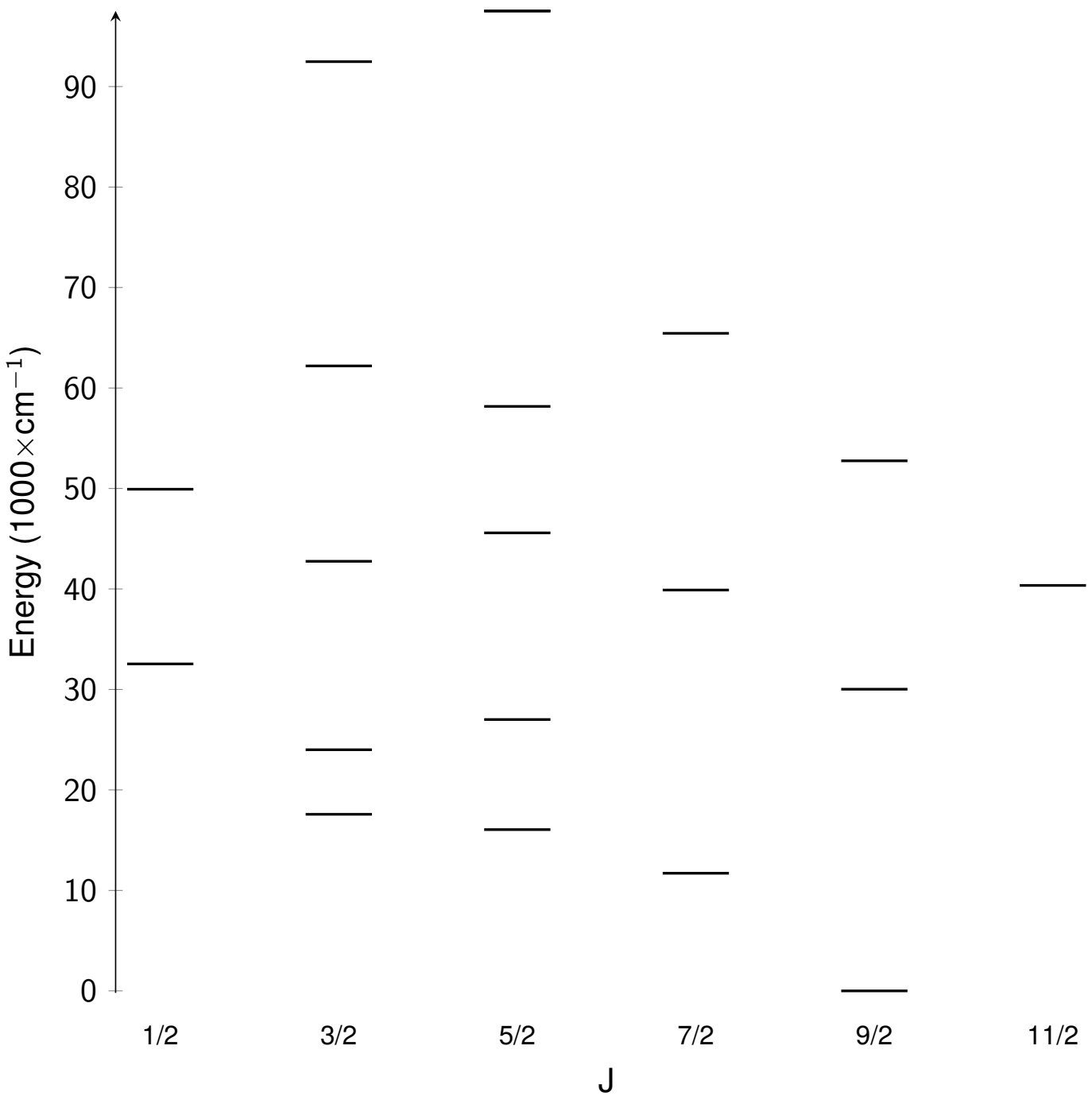


Fig. 7: Energy level diagram for all states of $[Kr]4d^7$ configuration of I^{10+} .

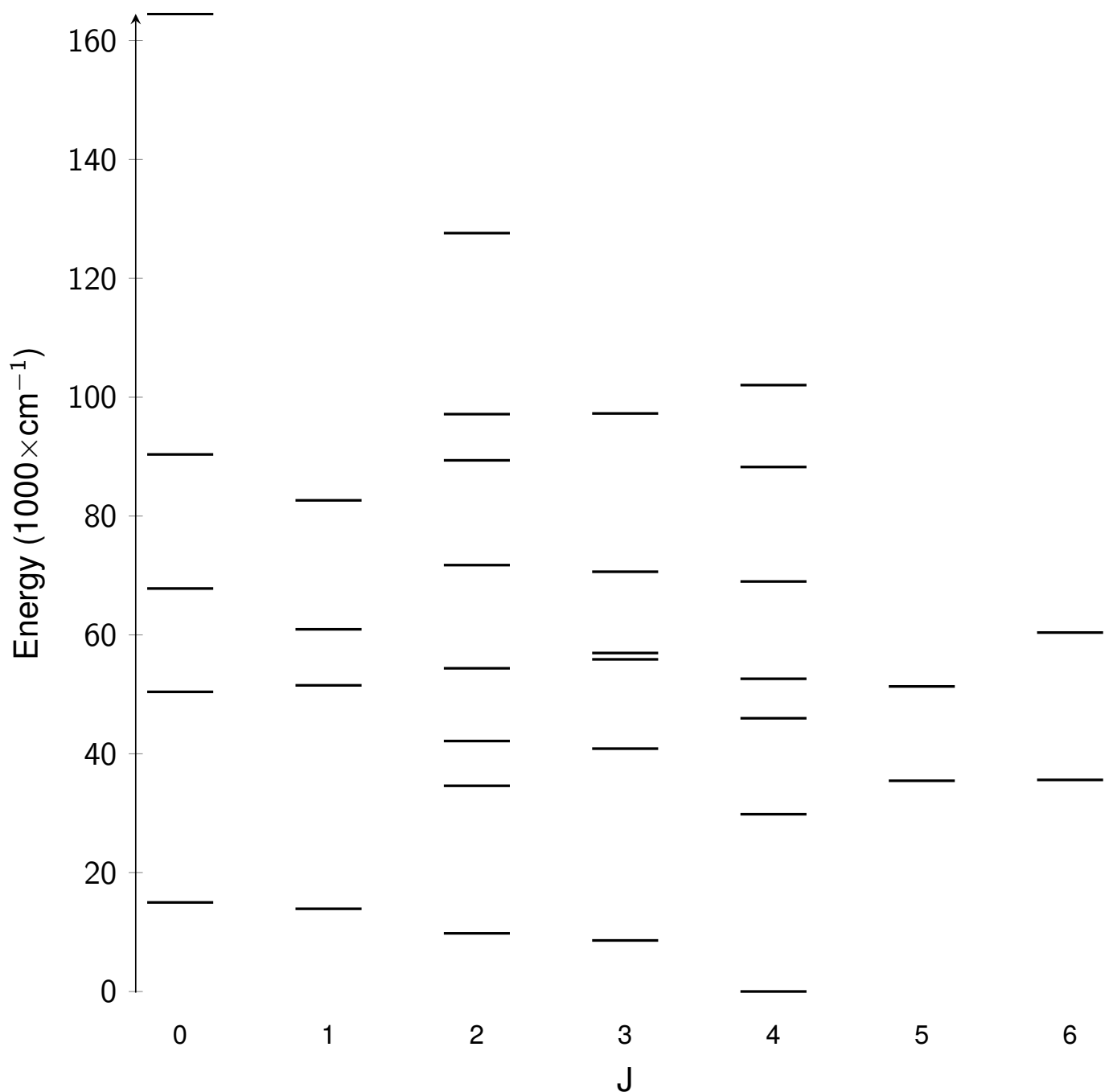


Fig. 8: Energy level diagram for all states of $[Kr]4d^6$ configuration of I^{11+} .

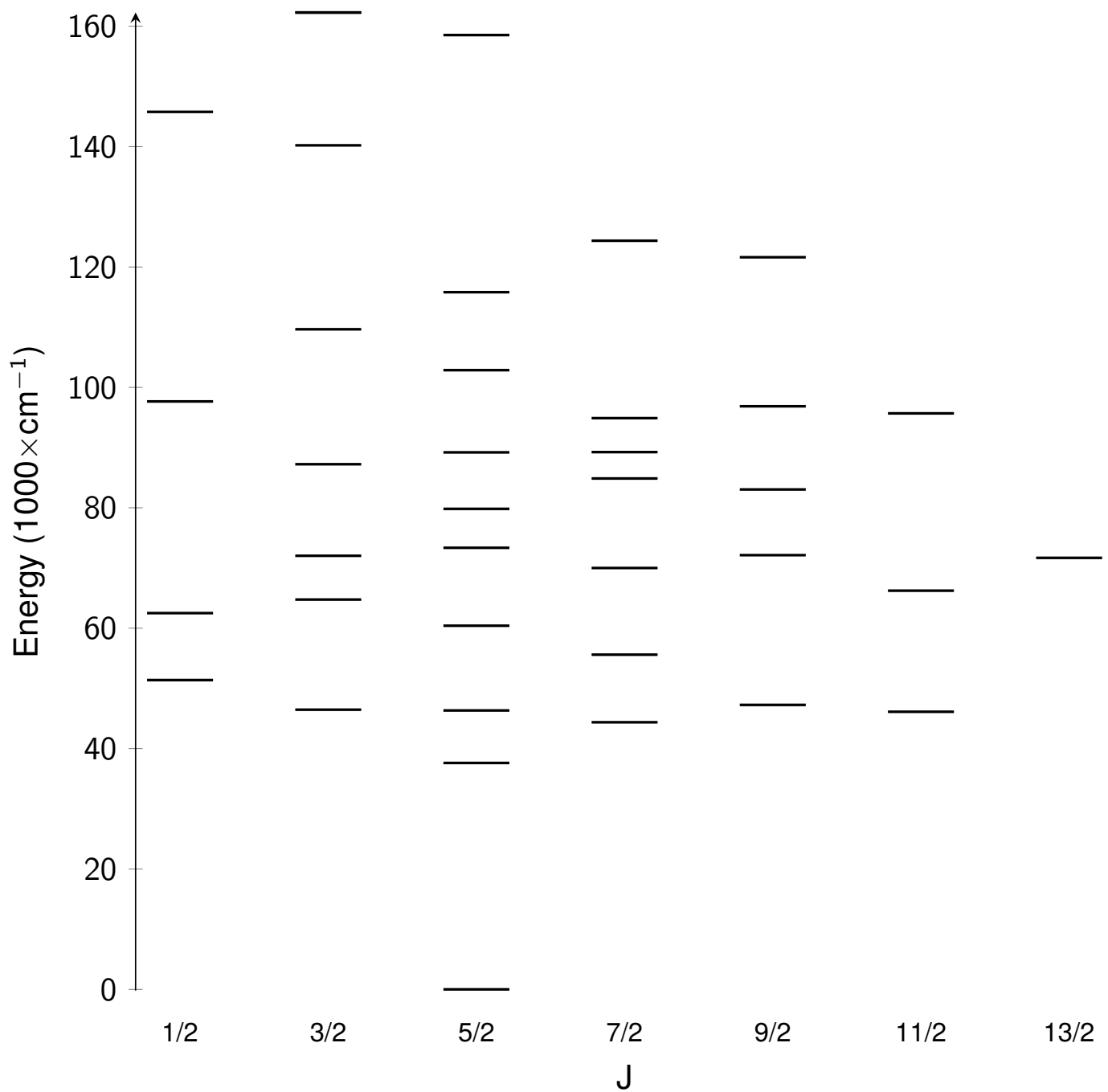


Fig. 9: Energy level diagram for all states of $[Kr]4d^5$ configuration of I^{12+} .